Controlling the Excited-State Dynamics of Low Band Gap, NIR Absorbers via Proquinoidal Unit Electronic Structural Modulation

Yusong Bai, Jeff Rawson, Sean A. Roget, Jean-Hubert Olivier, Jiaxing Lin, Peng Zhang, David N. Beratan, and Michael J. Therien*

Department of Chemistry, French Family Science Center, 124 Science Drive, Duke University, Durham, North Carolina 27708-0346, USA

Contents

1. Materials and Instrumentation

Materials. All manipulations were carried out under nitrogen or argon previously passed through an O_2 scrubbing tower (Schweitzerhall R3-11 catalyst) and a drying tower (Linde 3-Å molecular sieves) unless otherwise stated. Air sensitive solids were handled in a Braun 150-M glove box. Standard Schlenk techniques were employed to manipulate air-sensitive solutions. All solvents utilized in this work were obtained from Fisher Scientific (HPLC Grade). CH_2Cl_2 and tetrahydrofuran (THF) were distilled from CaH_2 and K/4-benzoylbiphenyl, respectively, under argon. Triethyleamine (TEA) was dried over KOH pellets and distilled under vacuum. All NMR solvents were used as received. The catalysts $Pd(PPh_3)_4$ and tris(dibenzylideneacetone)-dipalladium(0) (Pd_2dba_3), as well as triphenylarsine ($AsPh_3$),were purchased from Sigma-Aldrich. Various starting materials (Scheme S1), such as 4,9-bromo-6,7-dimethyl[1,2,5]thiadiazolo[3,4-g]quinoxaline (**Br-TDQ-Br**),[1] 4,7-diethynylbenzo[c][1,2,5]thiadiazole (**Br-BTD-Br**),[1-2] [5-triisopropylsilylethynyl-10,20-bis(2',6'-bis(3,3-dimethyl-1-butyloxy)phenyl)porphinato]zinc(II) (**ArPZnETIPS**), [5-ethynyl-10,20-bis(2',6'-bis(3,3-dimethyl-1-butyloxy)phenyl)porphinato]zinc(II) (**ArPZnE**),[3] [5-triisopropylsilylethynyl-10,15,20-tri(heptafluoropropyl)porphinato]zinc(II) (**Rf_3PZnETIPS**), and [5-ethynyl-10,15,20-tri(heptafluoropropyl)porphinato]zinc(II) (**Rf_3PZnE**)[4] were prepared according to the published procedures (Scheme S1). The synthesis of and NMR characterization of 4,9-bis[(10,20-bis[2',6'-bis(3,3-dimethyl-1-butyloxy)phenyl]porphinato)zinc(II)-5-ylethynyl]-6,7-dimethyl[1,2,5]thiadiazolo[3,4-g]quinoxaline (**ArPZnE-TDQ-EArPZn**) and 4,7-bis[(10,20-bis[2',6'-bis(3,3-dimethyl-1-butyloxy)phenyl]porphinato)zinc(II)-5-ylethynyl]benzo[c][1,2,5]thiadiazole (**ArPZnE-BTD-EArPZn**) have been reported previously (Scheme S1).[1] Flash and size exclusion column chromatography were performed on the bench top, using respectively silica gel (EM Science, 230–400 mesh) and Bio-Beads SX-1 as media.

Instrumentation. Electronic spectra were recorded on a Varian 5000 UV/vis/NIR spectrophotometry system. NMR spectra were recorded on a 400 MHz AC-Brucker instrument. Chemical shifts for ^{1}H NMR spectra are reported relative to residual protium in the deuterated solvents ($CDCl_3$ = 7.26 ppm, THF-d_8 = 1.72, 3.58 ppm). All J values are reported in Hertz. MALDI-TOF mass spectroscopic data were obtained with a Perspective Voyager DE Instrument (Department of Chemistry, Duke University). Samples were prepared as micromolar solutions in acetone, and 2-(4'-hydroxybenzeneazo)benzoic acid (Sigma-Aldrich) was utilized as the matrix. Microwave assisted reactions were performed with Emrys Personal Chemistry System (Biotage).

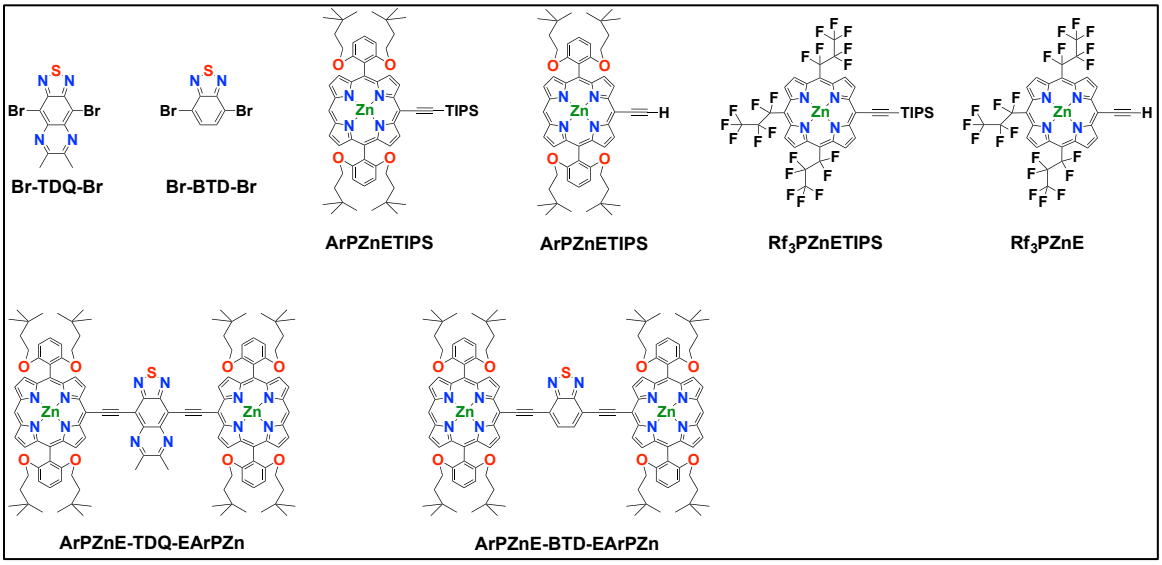

Scheme S1. Chemical structures of previously reported compounds, **Br-TDQ-Br**, **Br-BTD-Br**, **ArPZnETIPS**, **ArPZnE**, **Rf$_3$PZnETIPS**, **Rf$_3$PZnE**, **ArPZnE-TDQ-EArPZn**, and **ArPZnE-BTD-EArPZn**.

2. Synthetic Procedures and Characterization of New Chromophores

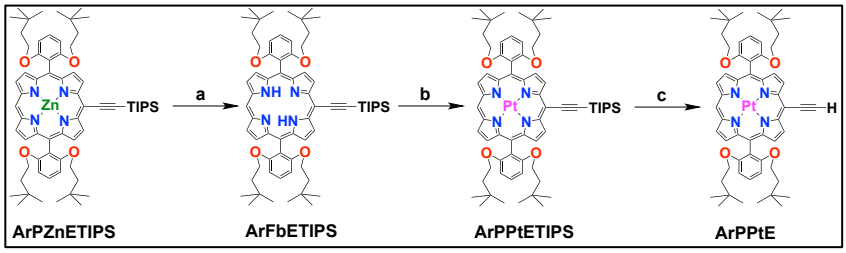

Scheme S2. Synthesis of **ArPPtE** from **ArPZnETIPS.** (a) trifluoroacetic acid, r.t., CH_2Cl_2, 30 min; (b) $Pt(acac)_2$, benzonitrile, 200 ^oC, 2h, microwave reaction; (c) TBAF, THF, 0 ^oC, 10 min, under argon.

5-Triisopropylsilylethynyl-10,20-bis(2',6'-bis(3,3-dimethyl-1-butyloxy)phenyl)porphyrin (**ArFbETIPS**). In a 100 mL round bottom flask equipped with a magnetic stirring bar, **ArPZnETIPS** (300 mg, 0.270 mmol) was dissolved by dry methylene chloride (~50 mL). Trifluoroacetic acid (5 mL) was added to the round bottom flask and the react was stirred at room temperature under argon for 0.5 h and then quenched by saturated $NaHCO_3$. The organic layer was collected, washed with saturated NH_4Cl, and then dried with Na_2SO_4. After evaporation of the solvent, the residue was purified by a short column chromatography using 1:1 hexanes: methylene chloride as the eluent. Yield = 275 mg (98 %, based on 300 mg of the **ArPZnETIPS** starting material). ^1H NMR (400MHz, $CDCl_3$ as 7.26 ppm): δ 10.02 (s, 1H), 9.67 (d, 2H, J = 4.8), 9.16 (d, 2H, J = 4.4 Hz), 8.87 (d, 2H, J = 4.8 Hz), 8.85 (d, 2H, J = 4.4 Hz), 7.71 (t, 2H, J = 8.4 Hz), 7.01 (d, 4H, J = 8.4 Hz), 3.91 (t, 8H, J = 7.2 Hz), 1.49-1.43 (m, 21H), 0.85 (t,

8H, J = 7.2 Hz), 0.32 (s, 36H), -2.56 (s, 2H). MALDI-TOF: m/z = 1045.65 (calculated for $C_{67}H_{91}N_4O_4Si$ $(M+H)^+$ 1045.57).

[5-Triisopropylsilylethynyl-10,20-bis(2',6'-bis(3,3-dimethyl-1-butyloxy)phenyl)porphinato]platinum(II) (**ArPPtETIPS**). **ArFbETIPS** (70 mg, 0.067 mmol), platinum acetylacetonate (132 mg, 0.335 mmol) and a magnetic stirring bar were brought together into a 10 mL microwave reaction vial that was then sealed and charged with argon. These reagents were dissolved in ~6 mL of benzonitrile solvent that was previously purged with argon for 1 h. The reaction vial was stirred at 200°C for 2 h in a microwave irradiation cavity. After the reaction without removing the benzonitrile solvent, the reaction mixture was directly purified through a silica column chromatography using 65:35 hexanes: methylene chloride eluent, and the first greenish band was collected as the desired product. Yield = 174 mg (70%, products from 3 reactions in total, based on 210 mg of the **ArFbETIPS** starting material). ^{1}H NMR (400MHz, $CDCl_3$ as 7.26 ppm): δ 9.92 (s, 1H), 9.58 (d, 2H, J = 4.8), 9.03 (d, 2H, J = 4.8 Hz), 8.80 (d, 2H, J = 4.8 Hz), 8.78 (d, 2H, J = 4.8 Hz), 7.69 (t, 2H, J = 8.4 Hz), 6.98 (d, 4H, J = 8.4 Hz), 3.90 (t, 8H, J = 7.2 Hz), 1.47-1.41 (m, 21H), 0.88 (t, 8H, J = 7.6 Hz), 0.24 (s, 36H). MALDI-TOF: m/z = 1235.36 (calculated for $C_{67}H_{91}N_4O_4PtSi$ $(M+H)^+$ 1237.63).

[5-Ethynyl-10,20-bis(2',6'-bis(3,3-dimethyl-1-butyloxy)phenyl)porphinato]platinum(II) (**ArPPtE**). Tetrabutylammonium fluoride (1M in THF, 126 μL, 0.126 mmol) was added to a solution of **ArPPtETIPS** (120 mg, 0.097 mmol) in THF (50 ml) under argon at 0°C. The reaction mixture was stirred for 10 min at 0 °C, quenched with water, extracted with CH_2Cl_2, dried over Na_2SO_4, and evaporated. The residue was chromatographed on silica gel using 85:15 hexanes:THF as the eluent. Yield = 100 mg (95%, based on 120 mg of **ArPPtETIPS**). ^{1}H NMR (400MHz, $CDCl_3$ as 7.26 ppm):): δ 9.93 (s, 1H), 9.59 (d, 2H, J = 4.8), 9.01 (d, 2H, J = 4.8 Hz), 8.82 (d, 2H, J = 4.8 Hz), 8.80 (d, 2H, J = 4.8 Hz), 7.66 (t, 2H, J = 8.4 Hz), 6.96 (d, 4H, J = 8.4 Hz), 4.13 (s, 1H), 3.90 (t, 8H, J = 7.2 Hz), 0.88 (t, 8H, J = 7.6 Hz), 0.24 (s, 36H). MALDI-TOF: m/z = 1082.12 (calculated for $C_{58}H_{70}N_4O_4Pt$ $(M+H)^+$ 1081.29).

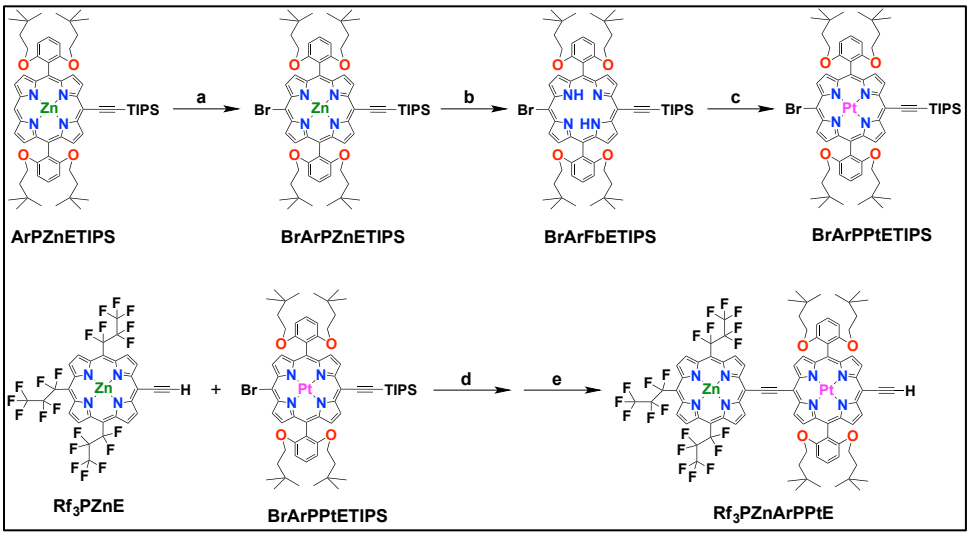

Scheme S3. Synthesis of **Rf$_3$PZnArPPtE** from **ArPZnETIPS** and **Rf$_3$PZnE**. (a) NBS, 0 ^{o}C, CH_2Cl_2:pyridine 20:1 mixture, 1 h, under argon; (b) trifluoroacetic acid, r.t., CH_2Cl_2, 30 min; (c) $Pt(acac)_2$, benzonitrile, 200 ^{o}C, 2h, microwave reaction; (d) $Pd_2(dba)_3$, $AsPh_3$, THF/*i*-Pr_2NH 10:1 mixture, 60 ^{o}C, 16 h, under argon; (e) TBAF, THF, 0 ^{o}C, 10 min, under argon.

[5-Bromo-15-triisopropylsilylethynyl-10,20-bis(2',6'-bis(3,3-dimethyl-1-butyloxy)phenyl)porphinato]zinc(II) (BrArPZnETIPS). In a 250 mL round bottom flask, **ArPZnETIPS** (180 mg, 0.163mmol) was dissolved in methylene chloride (50 mL) and pyridine (5 mL). The reaction mixture was cooled to 0 °C and a solution of NBS (32 mg, 0.179 mmol) in methylene chloride (50 mL) was added via cannula. The reaction mixture was stirred at 0 °C under argon for 1 h and quenched by addition of H_2O (100 mL). The organic layer was separated and dried with anhydrous Na_2SO_4. After evaporation of the solvent, the residue was purified by column chromatography using 6:4 hexanes: methylene chloride as the eluent. Yield = 155 mg (80 %, based on 180 mg of the **ArPZnETIPS** starting material). ^{1}H NMR (400MHz, $CDCl_3$ as 7.26 ppm): δ 9.72 (d, 2H, J = 4.4), 9.66 (d, 2H, J = 4.4), 8.93 (d, 2H, J = 4.4 Hz), 8.90 (d, 2H, J = 4.8 Hz), 7.74 (t, 2H, J = 8.4 Hz), 6.98 (d, 4H, J = 8.4 Hz), 3.96 (t, 8H, J = 7.2 Hz), 1.53-1.47 (m, 21H), 0.91 (t, 8H, J = 7.2 Hz), 0.32 (s, 36H). MALDI-TOF: m/z = 1184.57 (calculated for $C_{67}H_{88}BrN_4O_4SiZn$ $(M+H)^+$ 1186.83).

5-Bromo-15-triisopropylsilylethynyl-10,20-bis(2',6'-bis(3,3-dimethyl-1-butyloxy)phenyl)porphyrin (BrArFbETIPS). In a 100 mL round bottom flask equipped with a magnetic stirring bar, **BrArPZnETIPS** (120 mg, 0.101 mmol) was dissolved by dry methylene chloride (~50 mL). Trifluoroacetic acid (2 mL) was added to the round bottom flask and the react was stirred at room temperature under argon for 0.5 h and then quenched by saturated

$NaHCO_3$. The organic layer was collected, washed with saturated NH_4Cl, and then dried with Na_2SO_4. After evaporation of the solvent, the residue was purified by a short column chromatography using 1:1 hexanes: methylene chloride as the eluent. Yield = 111 mg (98 %, based on 120 mg of the **BrArPZnETIPS** starting material). ^{1}H NMR (400MHz, $CDCl_3$ as 7.26 ppm): δ 9.61 (d, 2H, J = 4.4), 9.54 (d, 2H, J = 4.4), 8.82 (d, 2H, J = 4.4 Hz), 8.78 (d, 2H, J = 4.8 Hz), 7.68 (t, 2H, J = 8.4 Hz), 6.91 (d, 4H, J = 8.4 Hz), 3.92 (t, 8H, J = 7.2 Hz), 1.53-1.47 (m, 21H), 0.89 (t, 8H, J = 7.2 Hz), 0.31 (s, 36H), -2.48 (s, 2H). MALDI-TOF: m/z = 1123.92 (calculated for $C_{67}H_{90}BrN_4O_4Si$ $(M+H)^+$ 1123.46).

[5-Bromo-15-triisopropylsilylethynyl-10,20-bis(2',6'-bis(3,3-dimethyl-1-butyloxy)phenyl)porphinato]platinum(II) (**BrArPPtETIPS**). **BrArFbETIPS** (70 mg, 0.062 mmol), platinum acetylacetonate (123 mg, 0.312 mmol) and a magnetic stirring bar were brought together into a 10 mL microwave reaction vial that was then sealed and charged with argon. These reagents were dissolved in ~6 mL of benzonitrile solvent that was previously purged with argon for 1 h. The reaction vial was stirred at 200^{o}C for 2 h in a microwave irradiation cavity. After the reaction without removing the benzonitrile solvent, the reaction mixture was directly purified through a silica column chromatography using 65:35 hexanes: methylene chloride eluent, and the first greenish band was collected as the desired product. Yield = 55 mg (68%, products from 3 reactions in total, based on 70 mg of the **BrArFbETIPS** starting material). ^{1}H NMR (400MHz, $CDCl_3$ as 7.26 ppm): δ 9.56 (d, 2H, J = 4.8), 9.51 (d, 2H, J = 4.8), 8.77 (d, 2H, J = 4.8 Hz), 8.75 (d, 2H, J = 4.8 Hz), 7.72 (t, 2H, J = 8.4 Hz), 7.01 (d, 4H, J = 8.4 Hz), 3.95 (t, 8H, J = 7.2 Hz), 1.51-1.44 (m, 21H), 0.95 (t, 8H, J = 7.2 Hz), 0.31 (s, 36H). MALDI-TOF: m/z = 1316.71 (calculated for $C_{67}H_{88}BrN_4O_4PtSi$ $(M+H)^+$ 1316.53).

1-[(5-,10,15,20-Tri(heptafluoropropyl)porphinato)zinc(II)]-2-[(5'-,15'-(triisopropylsilylethynyl)-10',20'-bis(2,6-bis(3,3-dimethyl-1-butyloxy)-phenyl)porphinato)platinum(II)]-ethyne (**Rf_3PZnArPPtETIPS**). A 100 mL Schlenk flask equipped with a magnetic stirbar was charged with **Rf_3PZnE** (60 mg, 0.067 mmol), **BrArPPtETIPS** (55 mg, 0.042 mmol), $Pd_2(dba)_3$ (23 mg, 0.025 mmol) and $AsPh_3$ (38 mg, 0.126 mmol). A solvent mixture of THF (50 mL) and diisopropylamine (5ml) was degassed via five freeze-pump-thaw cycles, transferred to the reaction flask and stirred at 60 °C for 16 h. After the reaction endpoint was confirmed by TLC, the reaction mixture was evaporated to dry and the

residue was sequentially purified by silica column chromatography using 1:1 hexanes: methylene chloride as the eluent, size exclusion column chromatography using THF as the eluent, and another silica column chromatography using 1:1 hexanes: methylene chloride as the eluent. Yield = 43 mg (48%, based on 55 mg of **BrArPPtETIPS**). ^{1}H NMR (400MHz, $CDCl_3$ as 7.26 ppm): δ 10.49 (d, 2H, J = 4.8), 10.12 (d, 2H, J = 4.8), 9.75 (s, 2H), 9.69 (s, 2H), 9.63 (s, 2H), 9.56 (d, 2H, J = 4.8), 8.99 (d, 2H, J = 4.8), 8.80 (d, 2H, J = 4.8), 7.73 (t, 2H, J = 8.4), 7.03 (d, 4H, J = 8.4), 3.99 (t, 8H, J = 7.2), 1.52-1.43 (m, 21H), 1.00 (t, 8H, J = 7.2), 0.33 (s, 36H). MALDI-TOF: m/z = 2138.19 (calculated for $C_{98}H_{96}F_{21}N_8O_8PtSiZn$ $(M+H)^+$ 2137.41).

1-[(5-,10,15,20-Tri(heptafluoropropyl)porphinato)zinc(II)]- 2-[(5'-,15'-(ethynyl)-10',20'-bis(2,6-bis(3,3-dimethyl-1-butyloxy)- phenyl)porphinato)platinum(II)]-ethyne (**Rf_3PZnArPPtE**). Tetrabutylammonium fluoride (1M in THF, 26 μL, 0.026 mmol) was added to a solution of **Rf_3PZnArPPtETIPS** (43 mg, 0.020 mmol) in THF (20 ml) under argon at 0°C. The reaction mixture was stirred for 10 min at 0 °C, quenched with water, extracted with CH_2Cl_2, dried over Na_2SO_4, and evaporated. The residue was chromatographed on silica gel using 85:15 hexanes:THF as the eluent. Yield = 38 mg (95%, based on 43 mg of **Rf_3PZnArPPtETIPS**). ^{1}H NMR (400MHz, $CDCl_3$ as 7.26 ppm): δ 10.47 (d, 2H, J = 4.8), 10.11 (d, 2H, J = 4.8), 9.73 (s, 2H), 9.67 (s, 2H), 9.61 (s, 2H), 9.55 (d, 2H, J = 4.8), 8.97 (d, 2H, J = 4.8), 8.78 (d, 2H, J = 4.8), 7.72 (t, 2H, J = 8.4), 7.03 (d, 4H, J = 8.4), 4.12 (s, 1H), 3.99 (t, 8H, J = 7.2), 0.98 (t, 8H, J = 7.2), 0.32 (s, 36H). MALDI-TOF: m/z = 1979.36 (calculated for $C_{89}H_{76}F_{21}N_8O_8PtZn$ $(M+H)^+$ 1981.06).

General Procedure for the Preparation of ArPPtE-TDQ-EArPPt, **ArPPtE-BTD-EArPPt**, **Rf_3PZnE-TDQ-ERf_3PZn**, and **Rf_3PZnArPPtE-TDQ-EArPPtRf_3PZn**. *meso*-ethynyl functionalized (porphinato)metal(II) derivatives (**ArPPtE**, **Rf_3PZnE**, and **Rf_3PZnArPPtE**) and proquinoidal spacer moieties (**Br-TDQ-Br**, and **Br-BTD-Br**) were placed in a Schlenk flask equipped with a magnetic stir bar. $Pd_2(dba)_3$ (0.3 eq., based on the (porphinato)zinc synthon) and $AsPh_3$ (2 eq., based on the (porphinato)zinc synthon) were added under nitrogen atmosphere. A solvent mixture of 10:1 HPLC grade THF:triethylamine was degassed by a small stream of dry argon for approximately 2 h. Enough of this solvent mixture was added to the reaction vessel via cannula to completely dissolve all reactants, and the resulting solution was heated to 50-60 °C for 16 h. Consumption of all the starting materials was confirmed by thin layer chromatography

(6:4 hexanes:CH_2Cl_2 as eluent for **ArPPtE-TDQ-EArPPt** and **ArPPtE-BTD-EArPPt**, 65:35 hexanes:THF as eluent for **Rf$_3$PZnE-TDQ-ERf$_3$PZn** and **Rf$_3$PZnArPPtE-TDQ-EArPPtRf$_3$PZn**). The solution was then cooled to room temperature and evaporated. The crude product was purified by column chromatography using 6:4 hexanes:CH_2Cl_2 as eluent for **ArPPtE-TDQ-EArPPt** and **ArPPtE-BTD-EArPPt**, 65:35 hexanes:THF as eluent (due to solubility reason) for **Rf$_3$PZnE-TDQ-ERf$_3$PZn** and **Rf$_3$PZnArPPtE-TDQ-EArPPtRf$_3$PZn**. The product fractions was concentrated to dryness, then further purified through size exclusion column chromatography (Bio-beads SX-1 medium) using THF as the eluent, followed by a short silica gel column chromatography using the corresponding solvent mixture as eluent (*vide supra*). Additional column chromatography was performed if the level of purity was unsatisfactory as assessed by NMR spectroscopy.

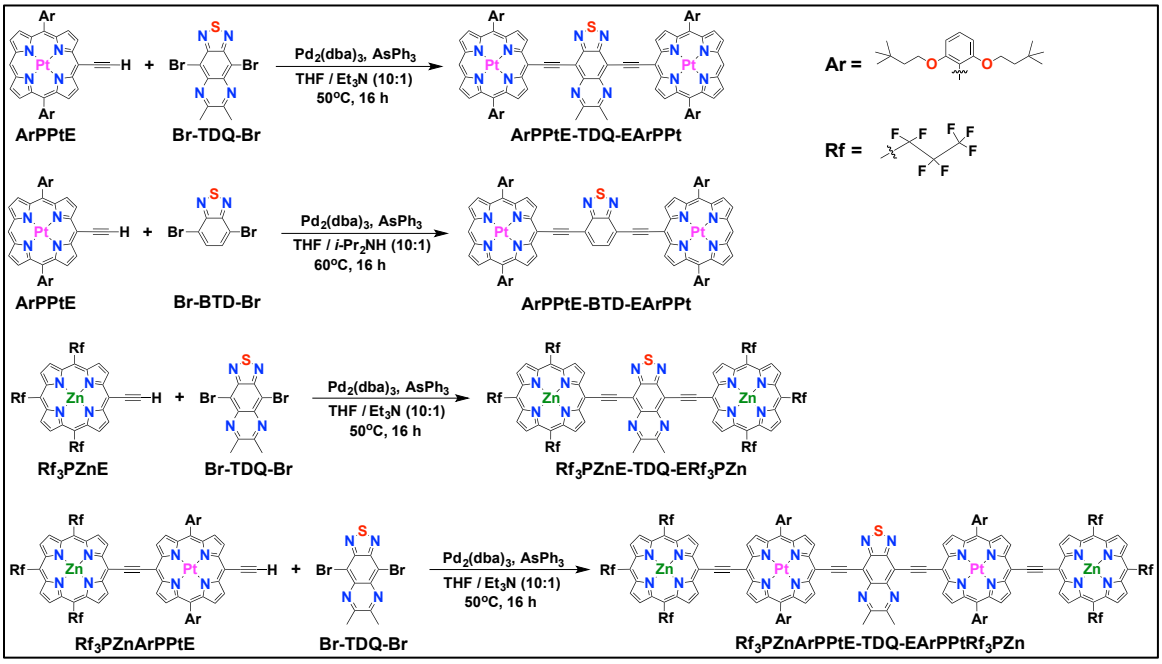

Scheme S4. Schematic summary for the synthesis of **ArPME-TDQ-EArPM**, **ArPME-BTD-EArPM** (**M** = **Zn^{II}**, or **Pt^{II}**), **Rf$_3$PZnE-TDQ-ERf$_3$PZn**, and **Rf$_3$PZnArPPtE-TDQ-EArPPtRf$_3$PZn**.

4,9-Bis[(10,20-bis[2',6'-bis(3,3-dimethyl-1-butyloxy)phenyl]porphinato)platinum(II)-5-ylethynyl]-6,7-dimethyl[1,2,5]thiadiazolo[3,4-g]quinoxaline (ArPPtE-TDQ-EArPPt). Reagents: **ArPPtE** (50 mg, 0.046 mmol), **Br-TDQ-Br** (9 mg, 0.023 mmol), $Pd_2(dba)_3$ (13 mg, 0.014 mmol), and $AsPh_3$ (28 mg, 0.092 mmol). Reaction solvent: 22 mL of 10:1 THF:triethylamine. Isolated yield = 30 mg of **ArPPtE-TDQ-EArPPt** (56%, based on 9 mg of **Br-TDQ-Br**). ^{1}H NMR (400MHz, $CDCl_3$ as 7.26 ppm): δ 10.39 (d, 4H, J = 4.8), 9.94 (s, 2H),

9.05 (d, 4H, J = 4.8), 8.98 (d, 4H, J = 4.8), 8.80 (d, 4H, J = 4.4), 7.76 (d, 4H, J = 8.4), 7.05 (d, 8H, J = 8.8), 3.97 (t, 16H, J = 7.2), 3.14 (s, 6H), 0.95 (t, 16H, J = 7.2), 0.25 (s, 72H). MALDI-TOF: m/z = 2371.35 (calculated for $C_{126}H_{141}N_{12}O_8Pt_2S$ $(M+H)^+$ 2373.81).

4,7-Bis[(10,20-bis[2',6'-bis(3,3-dimethyl-1-butyloxy)phenyl]porphinato)platinum(II)-5-ylethynyl]benzo[c][1,2,5]thiadiazole (**ArPPtE-BTD-EArPPt**). Reagents: **ArPPtE** (50 mg, 0.046 mmol), **Br-BTD-Br** (7 mg, 0.023 mmol), $Pd_2(dba)_3$ (13 mg, 0.014 mmol), and $AsPh_3$ (28 mg, 0.092 mmol). Reaction solvent: 22 mL of 10:1 THF:triethylamine. Isolated yield = 28 mg of **ArPPtE-BTD-EArPPt** (53%, based on 7 mg of **Br-BTD-Br**). ^{1}H NMR (400MHz, $CDCl_3$ as 7.26 ppm): δ 9.92 (d, 4H, J = 4.8), 9.80 (s, 2H), 8.94 (s, 4H), 8.92 (d, 4H, J = 4.8), 8.79 (d, 4H, J = 4.8), 7.98 (s, 2H), 7.75 (t, 4H, J = 8.4), 7.04 (d, 8H, J = 8.4), 3.97 (t, 16H, J = 7.2), 0.97 (t, 16H, J = 7.2), 0.26 (s, 72H). MALDI-TOF: m/z = 2294.81 (calculated for $C_{122}H_{137}N_{10}O_8Pt_2S$ $(M+H)^+$ 2293.72).

4,9-Bis[(10,15,20-Tri(heptafluoropropyl)porphinato)zinc(II)-5-ylethynyl]-6,7-dimethyl[1,2,5]thiadiazolo[3,4-g]quinoxaline (**Rf_3PZnE-TDQ-ERf_3PZn**). Reagents: **Rf_3PZnE** (42 mg, 0.046 mmol), **Br-TDQ-Br** (9 mg, 0.023 mmol), $Pd_2(dba)_3$ (13 mg, 0.014 mmol), and $AsPh_3$ (28 mg, 0.092 mmol). Reaction solvent: 22 mL of 10:1 THF:triethylamine. Isolated yield = 23 mg of **Rf_3PZnE-TDQ-ERf_3PZn** (50%, based on 9 mg of **Br-TDQ-Br**). ^{1}H NMR (400MHz, THF-d_8 as 1.72, 3.58 ppm): δ 10.35 (s, 4H), 9.68 (s, 4H), 9.60 (s, 4H), 9.32 (s, 4H), 3.28 (s, 6H). MALDI-TOF: m/z = 2014.76 (calculated for $C_{72}H_{23}F_{42}N_{12}SZn_2$ $(M+H)^+$ 2016.80).

4,9-Bis[[15-[(10',15',20'-tri(heptafluoropropyl)porphinato)zinc(II)-5'-ylethynyl]-10,20-bis(2',6'-bis(3,3-dimethyl-1-butyloxy)-phenyl)porphinato]platinum(II)-5-ylethynyl]-6,7-dimethyl[1,2,5]thiadiazolo[3,4-g]quinoxaline (**Rf_3PZnArPPtE-TDQ-EArPPtRf_3PZn**). Reagents: **Rf_3PZnE** (42 mg, 0.046 mmol), **Br-TDQ-Br** (9 mg, 0.023 mmol), $Pd_2(dba)_3$ (13 mg, 0.014 mmol), and $AsPh_3$ (28 mg, 0.092 mmol). Reaction solvent: 22 mL of 10:1 THF:triethylamine. Isolated yield = 23 mg of **Rf_3PZnArPPtE-TDQ-EArPPtRf_3PZn** (50%, based on 9 mg of **Br-TDQ-Br**). ^{1}H NMR (400MHz, THF-d_8 as 1.72, 3.58 ppm): δ 11.02 (d, 4H, J = 4.8), 10.66 (d, 4H, J = 4.8), 10.29 (s, 4H), 10.23 (s, 4H), 10.17 (s, 4H), 10.10 (d, 4H, J = 4.8), 9.53 (d, 4H, J = 4.8), 9.34 (d, 4H, J = 4.8), 8.27 (t, 4H, J = 8.4), 7.57 (d, 8H, J = 8.4), 4.53 (t,

16H, J = 7.2), 3.25 (s, 6H), 1.54 (t, 16H, J = 7.2), 0.89 (s, 72H). MALDI-TOF: m/z = 4174.16 (calculated for $C_{188}H_{155}F_{42}N_{20}O_8Pt_2SZn_2$ $(M+H)^+$ 4173.35).

3. Steady-State Emission Spectra

The emission spectroscopy for all the **PM-Sp-PM** supermolecular species were investigated at ambient temperature under both deoxygenated and oxygenated condition. Deoxygenation was achieved through three cycles of freeze-pump-thaw, oxygenation was done by purging with air for 30 min. The optical density at all the different excitation wavelengths is ≤ 0.1. For low-temperature experiments, prior to freezing the sample by liquid nitrogen, three cycles of freeze-pump-thaw was applied for deoxygenation.

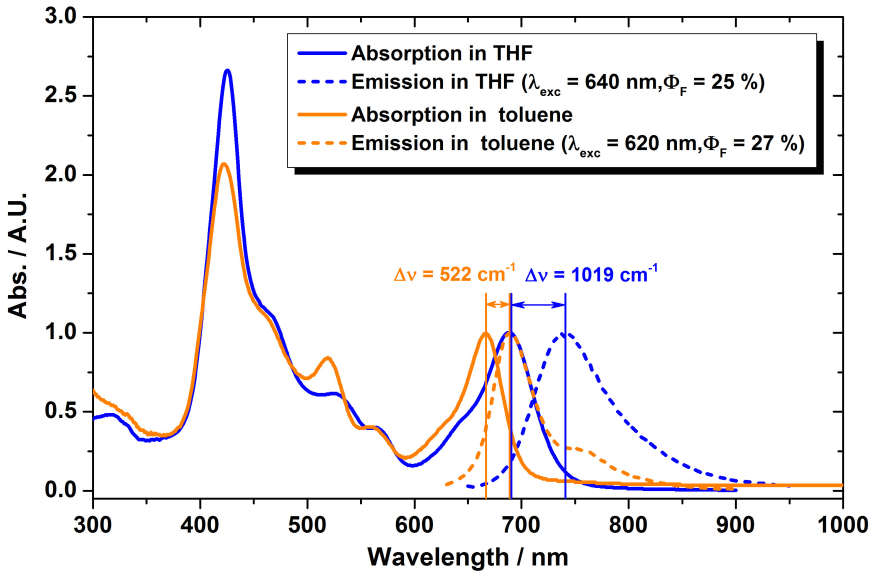

Figure S1. Comparative steady-state electronic absorption (solid lines) and emission spectra (dash lines) of **ArPZnE-BTD-EArPZn** in THF (blue lines) and toluene (orange lines). Stokes shift is computed based on the difference of the lowest-energy absorption and emission maxima.

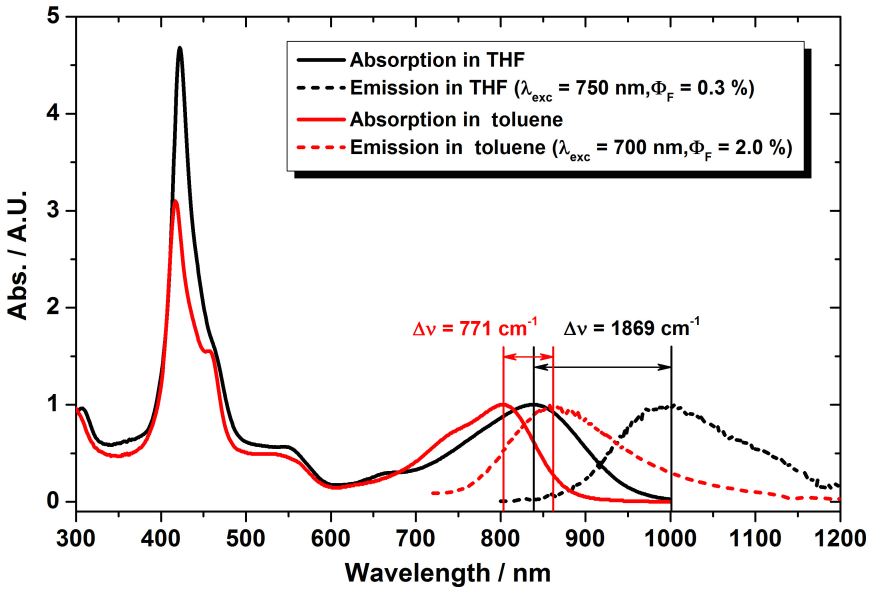

Figure S2. Comparative steady-state electronic absorption (solid lines) and emission spectra (dash lines) of **ArPZnE-TDQ-EArPZn** in THF (black lines) and toluene (red lines). Stokes shift is computed based on the difference of the lowest-energy absorption and emission maxima.

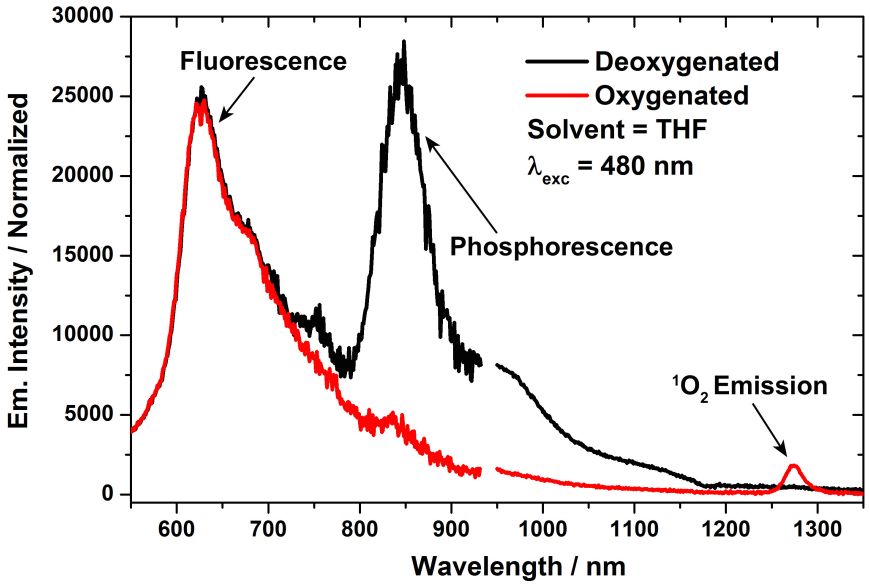

Figure S3. Steady-state emission spectra of **ArPPtE-BTD-EArPPt** measured under deoxygenated (black line) and oxygenated (red line) condition. Experimental conditions: λ_{exc} = 480 nm, ambient temperature, solvent = THF.

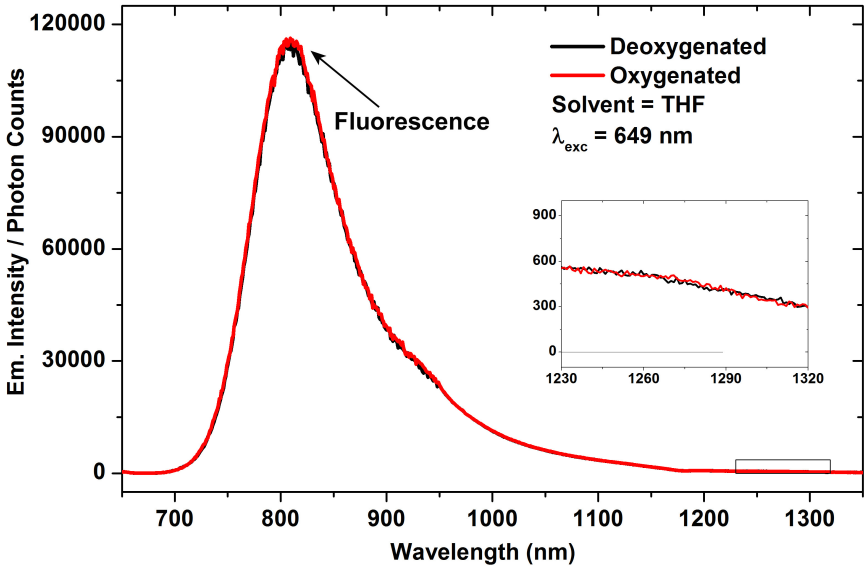

Figure S4. Steady-state emission spectra of **ArPPtE-TDQ-EArPPt** measured at deoxygenated (black line) and oxygenated (red line) condition. Experimental conditions: λ_{exc} = 649 nm, ambient temperature, solvent = THF.

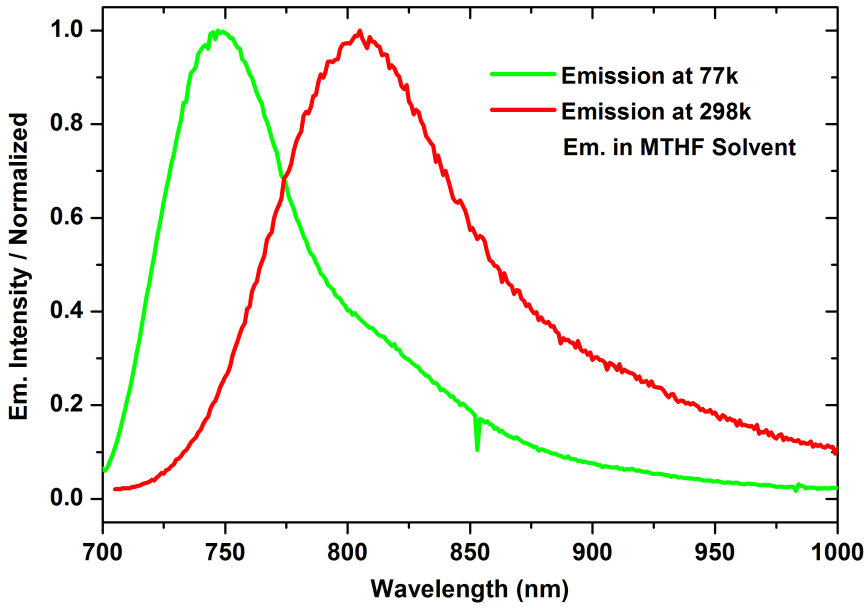

Figure S5. Steady-state emission spectra of **ArPPtE-TDQ-EArPPt** measured at low temperature (77K, green line) and room temperature (298K, red line). Experimental conditions: λ_{exc} = 649 nm, solvent = Methyl-THF.

4. Picosecond Fluorescence Lifetime Results

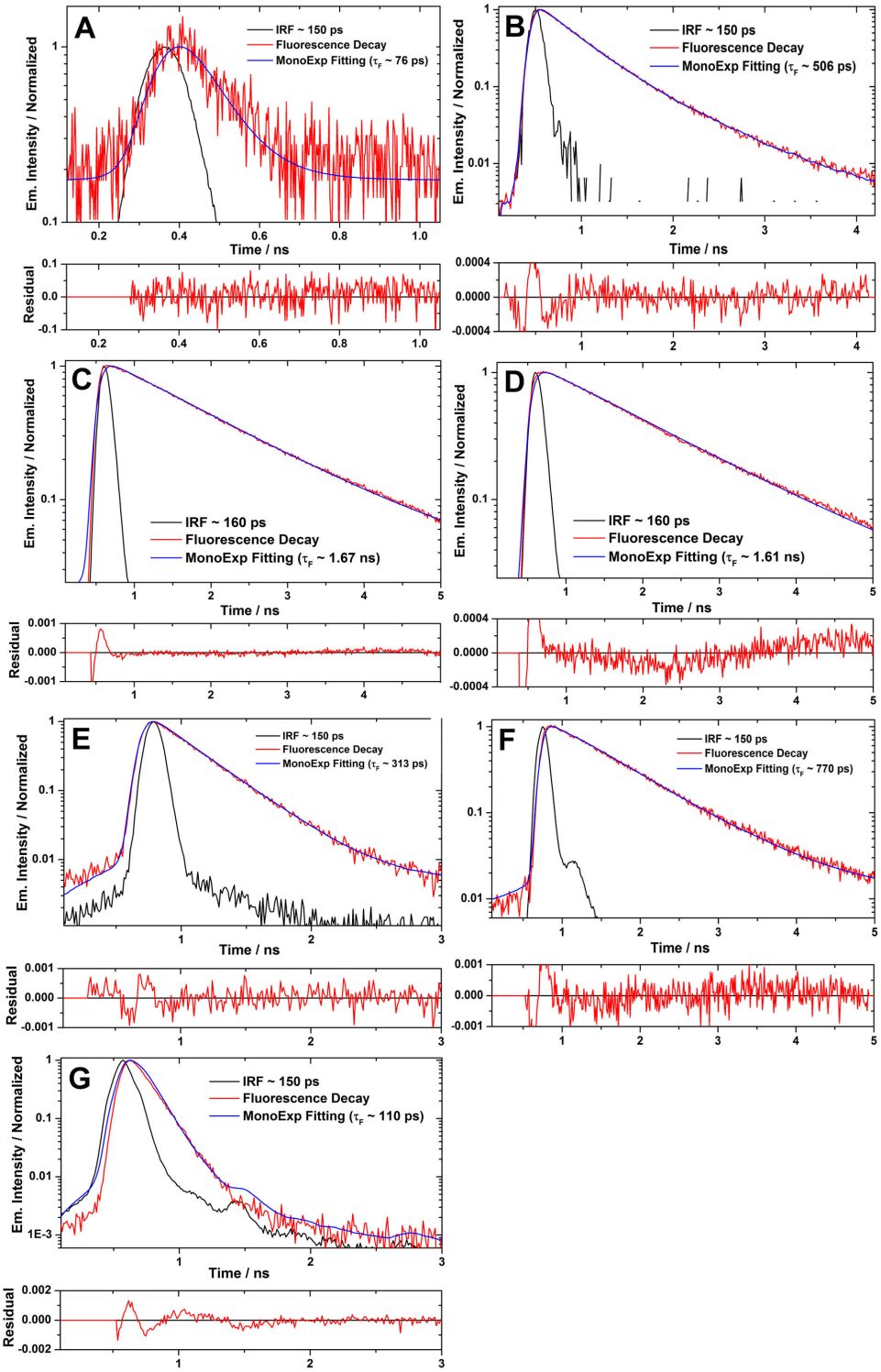

Figure S6. Picosecond fluorescence decay of **ArPZnE-TDQ-EArPZn** in THF (A) and toluene (B), **ArPZnE-BTD-EArPZn** in THF (C) and toluene (D), **ArPPtE-TDQ-EArPPt** in THF (E), **Rf$_3$PZnE-TDQ-ERf$_3$PZn** in THF (F), and **Rf$_3$PZnArPPtE-TDQ-EArPPtRf$_3$PZn** in THF (G). Experimental conditions: λ_{exc} = 405 nm, instrument response function (IRF) ~ 150-160 ps, ambient temperature, magic angle polarization.

5. Nanosecond-to-Microsecond Transient Absorption and Triplet Excited-State Lifetime.

Nanosecond-to-microsecond transient absorption for all chromophores were measured with air-free spectro-cell, three cycles of freeze-pump-thaw was applied for deoxygenation prior to measurement. Oxygen quenching experiments were performed by purging the sample with air for ~ 30 min before measurement. Kinetic traces were fitted with single-exponential decay model to acquire the excited triplet state lifetime.

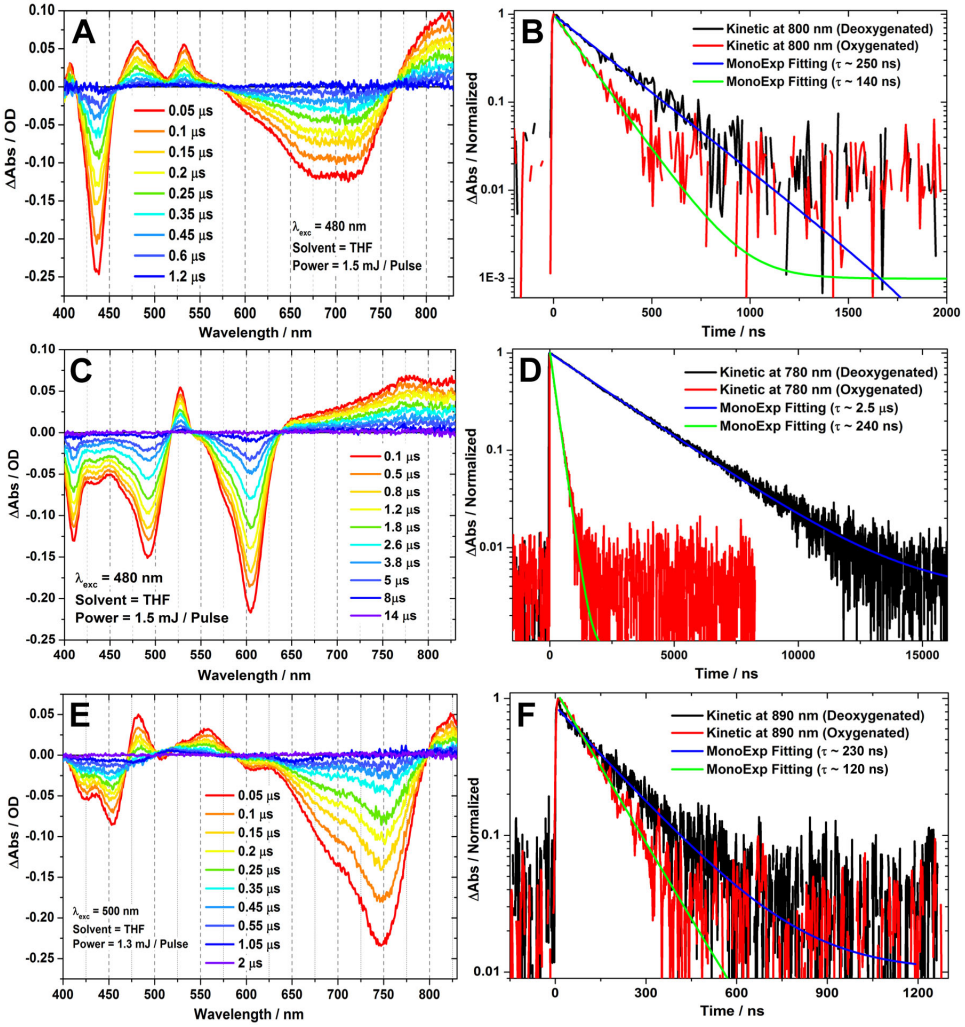

Figure S7. Nanosecond-to-microsecond transient absorption spectra recorded at selected time delays (under deoxygenated condition) and transient kinetic traces (under deoxygenated and oxygenated condition, respectively) for **ArPPtE-TDQ-EArPPt** (A) and (B), **ArPPtE-BTD-EArPPt** (C) and (D), and **Rf$_3$PZnArPPtE-TDQ-EArPPtRf$_3$PZn** (E) and (F). Experimental condition: λ_{exc} = 480 nm (**ArPPtE-TDQ-EArPPt**, **ArPPtE-BTD-EArPPt**), 500 nm (**Rf$_3$PZnArPPtE-TDQ-EArPPtRf$_3$PZn**), pump power = 1.5 mJ / pulse (**ArPPtE-TDQ-EArPPt**, **ArPPtE-BTD-EArPPt**), 1.3 mJ / pulse (**Rf$_3$PZnArPPtE-TDQ-EArPPtRf$_3$PZn**), solvent = THF, ambient temperature.

6. Other Supplementary Spectra.

6.1 Global Fitting and Decay Associated Difference Spectra

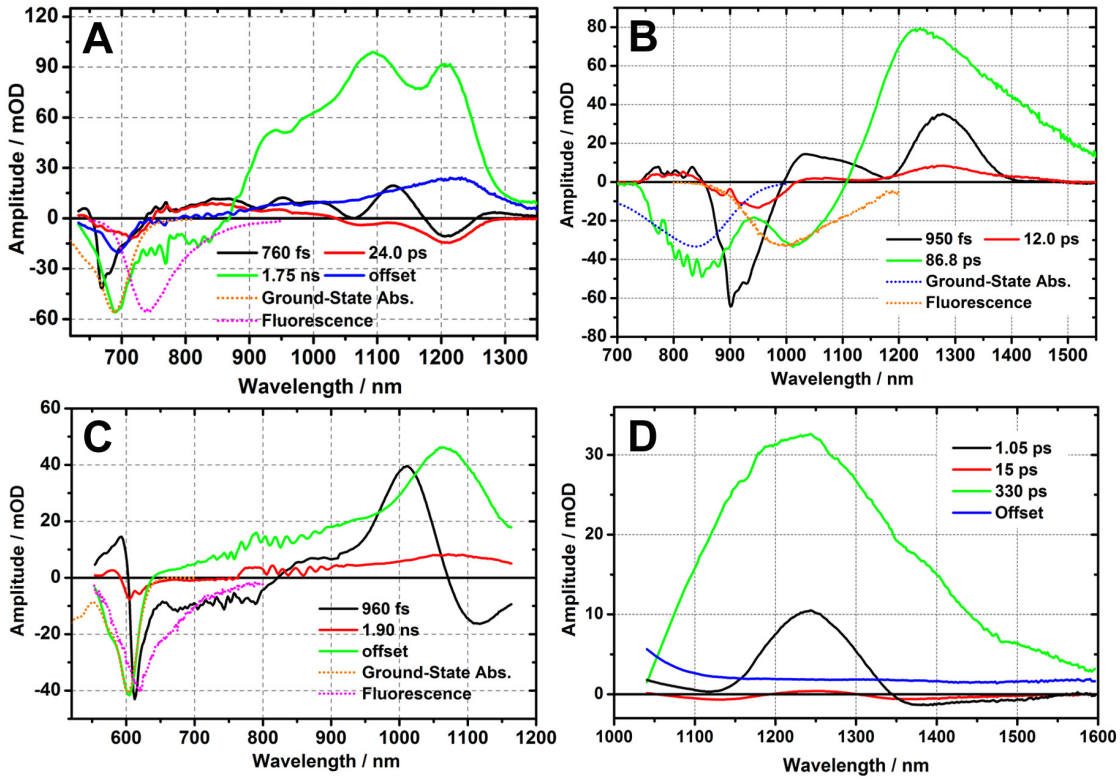

Figure S8. DADS of the NIR regime for **ArPZnE-BTD-EArPZn** (A), **ArPZnE-TDQ-EArPZn** (B), **ArPPtE-BTD-EArPPt** (C), and **ArPPtE-TDQ-EArPPt** (D), revealing solvent relaxation dynamic (~ 1 ps), structural (torsional) relaxation dynamics (~ 10-30 ps), and the intrinsic S_1 state decay. Offsets account for the transient absorption signal of the evolved excited triplet states, which persists beyond the delay limit of the transient optical system. Steady-state absorption and emission are plotted as the inverted dash lines.

6.2 Estimation of ISC Quantum Yields for ArPPtE-TDQ-EArPPt

The *ISC* quantum yield for **ArPPtE-TDQ-EArPPt** was determined from fs transient absorption spectral data via comparison of spectra acquired at t = 30 ps, which probes the excited singlet population without influence from solvent and structural relaxation dynamics (these processes are in the time domain of ~ 1 ps and 10-30 ps), and at a delay time (*e.g.*, t = 1.32 ns) at which only ground and excited triplet state populations of **ArPPtE-TDQ-EArPPt** exist. The ISC quantum yield can be estimated using equation (1).

$$\Phi_{ISC} = \frac{\Delta A\ (715\ nm, t{=}1.32\ ns)}{\Delta A\ (715\ nm, t{=}30\ ps)} \qquad (1)$$

To ensure the accuracy of the calculated Φ_{ISC}, the ΔA utilized in equation (1) has to be a pure

signal from ground state bleach (GSB). In this regard, note that the *Q*-band region (600-800 nm) GSB at t = 30 ps overlaps well with the ground-state absorption (Figure S9A), and due to the large Stokes shift, stimulated emission signal is greatly separated from the GSB signal, suggesting ΔA (715 nm, t = 30 ps) can be attributed only to the depletion of ground state populations (due to excited singlet populations). However, the *Q*-band region GSB at t = 1.32 ns does not overlap with the ground-state absorption (Figure S9A), particular in the spectral domain of 700-800 nm that is due to the triplet excited state absorption. To eliminate the influence from the triplet excited state absorption on the *Q*-band region GSB at t = 1.32 ns, spectra deconvolution is required. The *Q*-band ground-state electronic absorption can be deconvoluted using three Gaussian peaks (Figure S9B), therefore, a similar deconvolution pattern was utilized for *Q*-band region GSB at t = 1.32 ns (Figure S9C, Fit Peak 3-5). Another two Gaussian peaks that account for the triplet excited state absorption were required to fit transient absorption spectra (t = 1.32 ns) in the 575-1075 nm spectral domain (Figure S9C, Fit Peak 1-2). Thus, the pure signal from *Q*-band region GSB at t = 1.32 ns can be acquired by addition of the three negative Gaussian peaks in Figure S9C (Fit Peak 3-5), and ΔA (715 nm, t = 1.32 ns) obtained based on such deconvoluted spectra can be attributed only to the depletion of ground state populations (due excited triplet populations) (Figure S9D). Then, Φ_{ISC} (**ArPPtE-TDQ-EArPPt**) = ΔA (715 nm, t = 1.32 ns) / ΔA (715 nm, t = 30 ps) = (-28.66 mOD) / (-14.37 mOD) = 0.5. In the similar manner, the Φ_{ISC} for **Rf$_3$PZnArPPtE-TDQ-EArPPtRf$_3$PZn** can also be calculated, resulting in Φ_{ISC} (**Rf$_3$PZnArPPtE-TDQ-EArPPtRf$_3$PZn**) = 0.73.

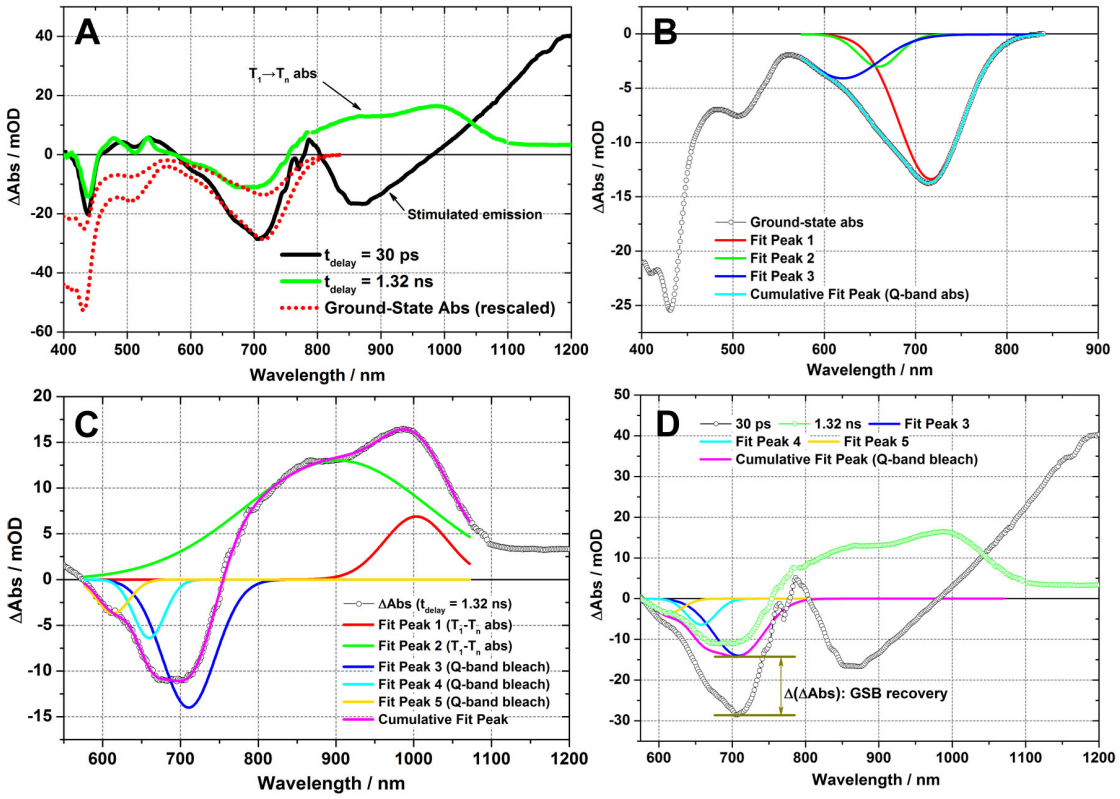

Figure S9. Spectral deconvolution for transient absorption at t = 1.32 ns. Comparative spectra among ground-state electronic absorption (red dotted lines, rescaled), transient absorption at t = 30 ps (black solid line), and transient absorption at t = 1.32 ns (green solid line) (A). Spectral deconvolution of *Q*-band ground-state electronic absorption (B). Spectra deconvolution of transient absorption at t = 1.32 ns in the spectral domain of 575-1075 nm. *Q*-band region ground state bleach recovery calculations (D).

6.3 Dynamic Stokes Shift in Ultrafast Time Domain

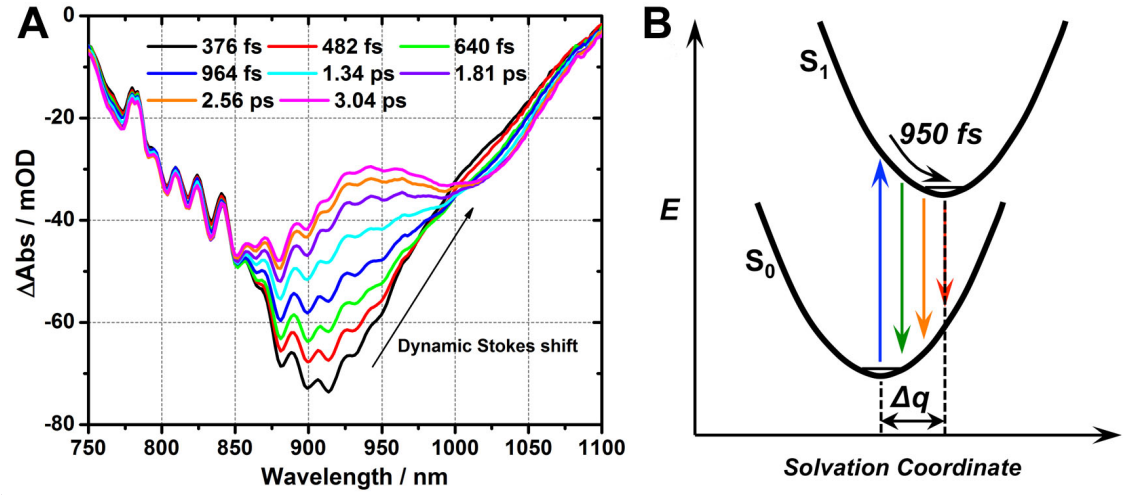

Figure S10. (A) Femtosecond transient absorption spectra of *Q*-band bleach and stimulated emission region in the time domain of solvation dynamics, experimental condition: λ_{exc} = 900 nm, power = 260 nJ / pulse, solvent = THF, ambient temperature, magic angle polarization. (B) Schematic illustration of dynamics Stokes shift of **ArPZnE-**

TDQ-EArPZn in THF, where potential energy curve displacement (Δq) between S_0 and S_1 states along the solvation coordinate plays a key role.

7. TD-DFT Calculations and Population Analysis

All calculations were performed upon structures with aliphatic chains truncated to methyl groups (Figure S59, molecular structures on top). For these oligo(porphinato)metal(II) species, C_{2V} conformeric minima could be formulated. Ground-state structure optimizations were performed with Density Functional Theory (DFT) using Gaussian 09, Rev C.1.[5] The M11[6] functional was employed for all calculations. Optimizations were performed with minimal symmetry constraints using tight optimization criteria; initial optimizations used smaller basis sets but the final optimizations and TD-DFT calculations employed the 6-311g(d) basis set[7] as implemented in Gaussian 09. TD-DFT result files were post-processed using the GaussSum package;[6] this software partitions the wavefunction amplitudes onto molecule fragments using Mulliken population analysis.[8]

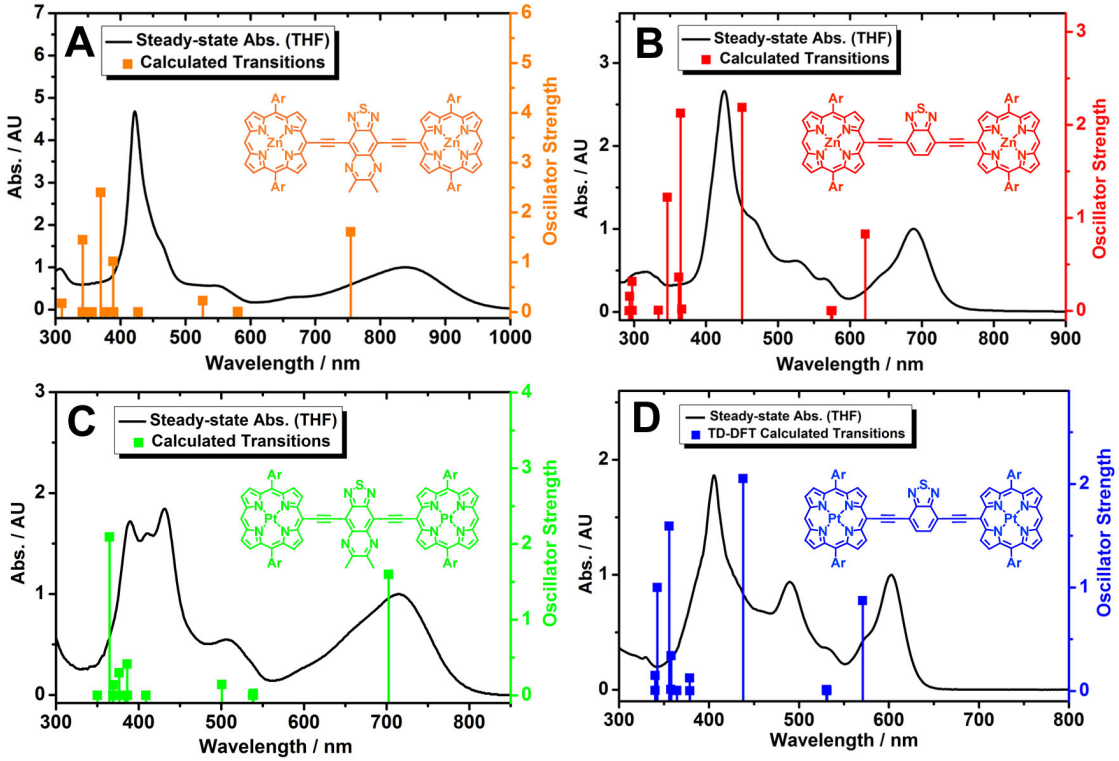

Figure S11. Comparison of TD-DFT predicted transitions and experimentally determined ground-state absorption spectra for **ArPZnE-TDQ-EArPZn** (A), **ArPZnE-BTD-EArPZn** (B), **ArPPtE-TDQ-EArPPt** (C), and **ArPPtE-BTD-EArPPt** (D).

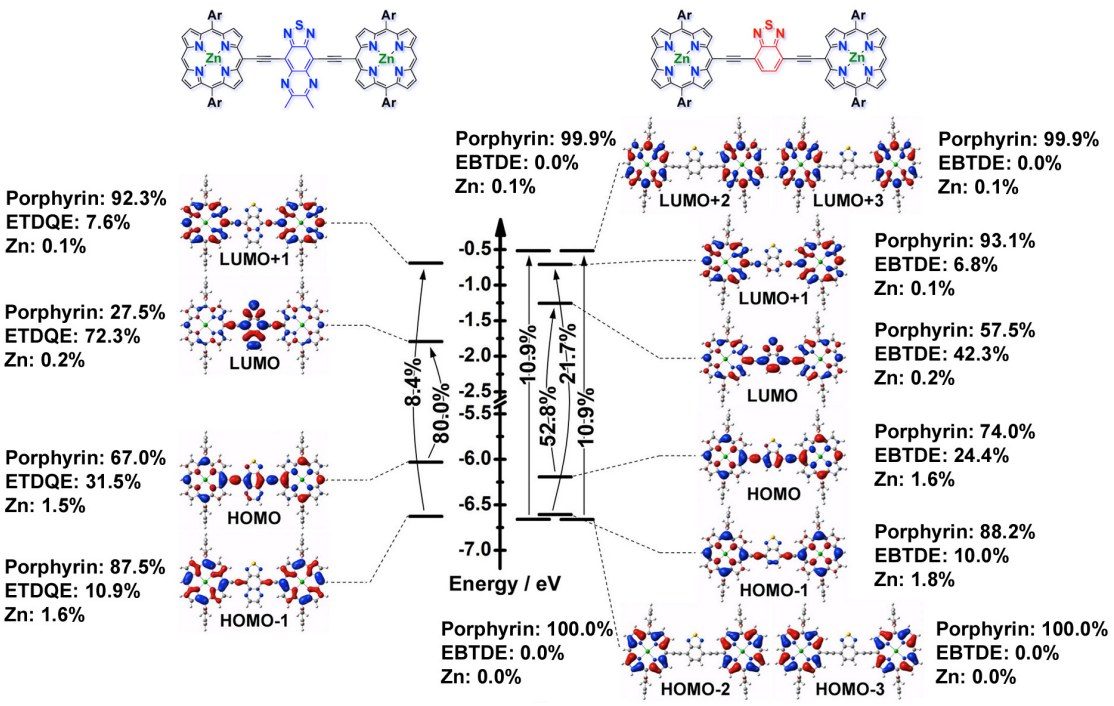

Figure S12. Frontier orbitals plotted as 0.02 isodensity surfaces for (left) **ArPZnE-TDQ-EArPZn** and (right) **ArPZnE-BTD-EArPZn**, along with a diagram comparing their calculated energies. Arrows depict the major one-electron configurations with percentages representing each excitation's contribution to the lowest-energy transition. The coefficients of each molecular orbital contributed by porphyrin, spacers (**ETDQE** and **EBTDE**), and zinc atoms are listed, determined by population analysis.

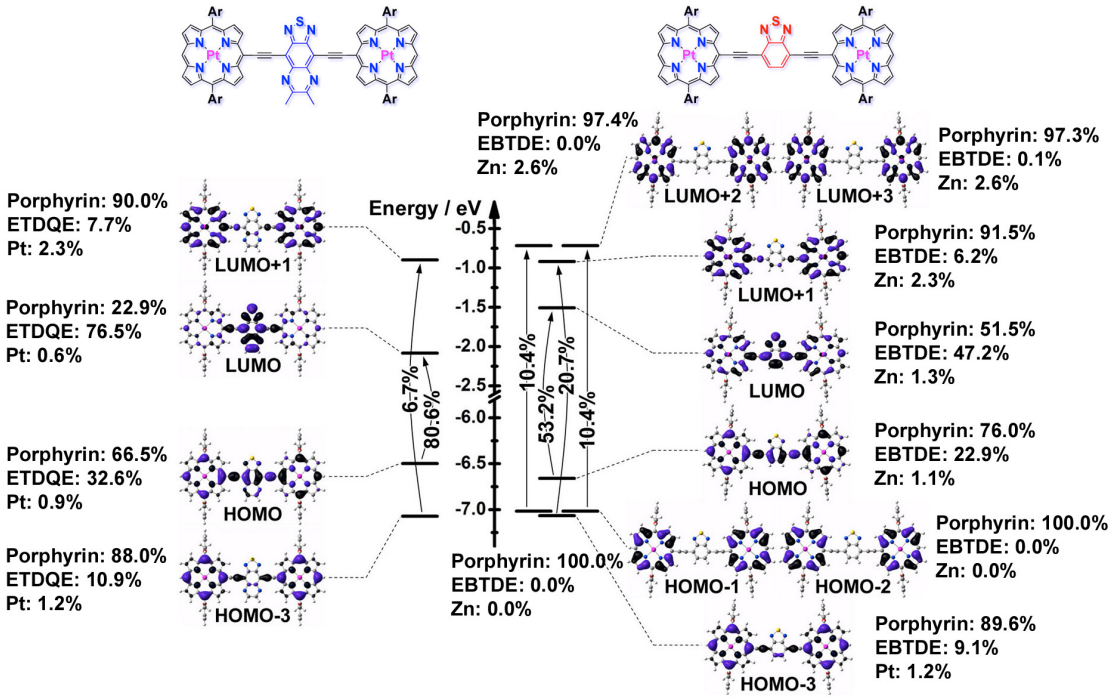

Figure S13. Frontier orbitals plotted as 0.02 isodensity surfaces for (left) **ArPPtE-TDQ-EArPPt** and (right) **ArPPtE-BTD-EArPPt**, along with a diagram comparing their calculated energies. Arrows depict the major one-electron configurations with percentages representing each excitation's contribution to the lowest-energy transition.

The coefficients of each molecular orbital contributed by porphyrin, spacers (**ETDQE** and **EBTDE**), and zinc atoms are listed, determined by population analysis.

References:

(1) Susumu, K.; Duncan, T. V.; Therien, M. J. *J. Am. Chem. Soc.* **2005**, *127*, 5186-5195.
(2) (a) Jin, Y.; Kim, Y.; Kim, S. H.; Song, S.; Woo, H. Y.; Lee, K.; Suh, H. *Macromolecules* **2008**, *41*, 5548-5554. (b) Kim, J. H.; Kim, H. U.; Mi, D.; Jin, S. H.; Shin, W. S.; Yoon, S. C.; Kang, I. N.; Hwang, D. H. *Macromolecules* **2012**, *45*, 2367-2376. (c) Neto, B. A. D.; Lopes, A. S. A.; Ebeling, G.; Goncalves, R. S.; Costa, V. E. U.; Quina, F. H.; Dupont, J. *Tetrahedron* **2005**, *61*, 10975-10982. (d) Wang, B.; Tsang, S. W.; Zhang, W. F.; Tao, Y.; Wong, M. S. *Chem. Commun.* **2011**, *47*, 9471-9473.
(3) (a) Duncan, T. V.; Frail, P. R.; Miloradovic, I. R.; Therien, M. J. *J. Phys. Chem. B* **2010**, *114*, 14696-14702. (b) Duncan, T. V.; Ishizuka, T.; Therien, M. J. *J. Am. Chem. Soc.* **2007**, *129*, 9691-9703. (c) Lin, V. S.-Y.; DiMagno, S. G.; Therien, M. J. *Science* **1994**, *264*, 1105-1111. (d) Lin, V. S.-Y.; Therien, M. J. *Chem. Eur. J.* **1995**, *1*, 645-651. (e) Susumu, K.; Therien, M. J. *J. Am. Chem. Soc.* **2002**, *124*, 8550-8552.
(4) Rawson, J.; Therien, M. J. Manuscript in preparation.
(5) Frisch, M. J.; Trucks, G. W.; Schlegel, H. B.; Scuseria, G. E.; Robb, M. A.; Cheeseman, J. R.; Scalmani, G.; Barone, V.; Mennucci, B.; Petersson, G. A.; Nakatsuji, H.; Caricato, M.; Li, X.; Hratchian, H. P.; Izmaylov, A. F.; Bloino, J.; Zheng, G.; Sonnenberg, J. L.; Hada, M. E., M.; Toyota, K.; Fukuda, R.; Hasegawa, J.; Ishida, M.; Nakajima, T.; Honda, Y.; Kitao, O.; Nakai, H.; Vreven, T.; Montgomery, J. A.; Peralta, J. E.; Ogliaro, F.; Bearpark, M.; Heyd, J. J.; Brothers, E.; Kudin, K. N.; Staroverov, V. N.; Kobayashi, R.; Normand, J.; Raghavachari, K.; Rendell, A.; Burant, J. C.; Iyengar, S. S.; Tomasi, J.; Cossi, M.; Rega, N.; Millam, J. M.; Klene, M.; Knox, J. E.; Cross, J. B.; Bakken, V.; Adamo, C.; Jaramillo, J.; Gomperts, R.; Stratmann, R. E.; Yazyev, O.; Austin, A. J.; Cammi, R.; Pomelli, C.; Ochterski, J. W.; Martin, R. L.; Morokuma, K.; Zakrzewski, V. G.; Voth, G. A.; Salvador, P.; Dannenberg, J. J.; Dapprich, S.; Daniels, A. D.; Farkas, Ö.; Foresman, J. B.; Ortiz, J. V.; Cioslowski, J.; Fox, D. J.; Rev. C.1. ed.; Gaussian, Inc.: Wallingford CT, 2009.
(6) O'Boyle, N. M.; Tenderholt, A. L.; Langner, K. M. *J. Comput. Chem.* **2008**, *29*, 839-845.
(7) (a) Wachters, A. J. *J. Chem. Phys.* **1970**, *52*, 1033-1036. (b) Hay, P. J. *J. Chem. Phys.* **1977**, *66*, 4377-4384. (c) Krishnan, R.; Binkley, J. S.; Seeger, R.; Pople, J. A. *J. Chem. Phys.* **1980**, *72*, 650-654. (d) Mclean, A. D.; Chandler, G. S. *J. Chem. Phys.* **1980**, *72*, 5639-5648. (e) Raghavachari, K.; Trucks, G. W. *J. Chem. Phys.* **1989**, *91*, 1062-1065. (f) Binning, R. C.; Curtiss, L. A. *J. Comput. Chem.* **1990**, *11*, 1206-1216. (g) Mcgrath, M. P.; Radom, L. *J. Chem. Phys.* **1991**, *94*, 511-516. (h) Curtiss, L. A.; Mcgrath, M. P.; Blaudeau, J. P.; Davis, N. E.; Binning, R. C.; Radom, L. *J. Chem. Phys.* **1995**, *103*, 6104-6113. (i) Blaudeau, J. P.; McGrath, M. P.; Curtiss, L. A.; Radom, L. *J. Chem. Phys.* **1997**, *107*, 5016-5021.
(8) Mulliken, R. S. *J. Chem. Phys.* **1955**, *23*, 1833-1840.